Inhibitory effects of umbelliferone on carbon tetrachloride-induced hepatic fibrosis in rats through the TGF-β1-Smad signaling pathway

LIJUAN LIANG[1*], ZHIHENG DONG[2*], ZIQING SHEN[1], YIFAN ZANG[1], WENLONG YANG[1], LAN WU[3] and LIDAO BAO[4]

[1]College of Pharmacy, Inner Mongolia Medical University, Hohhot, Inner Mongolia Autonomous Region 010110, P.R. China; [2]Department of Pharmacy, Affiliated Hospital of Inner Mongolia Medical University, Hohhot, Inner Mongolia Autonomous Region 010030, P.R. China; [3]Mongolia Medical School, Inner Mongolia Medical University, Hohhot, Inner Mongolia Autonomous Region 010110, P.R. China; [4]Department of Pharmacy, Hohhot First Hospital, Hohhot, Inner Mongolia Autonomous Region 010030, P.R. China

Received January 14, 2025; Accepted March 19, 2025

DOI: 10.3892/mmr.2025.13536

Abstract. Hepatic fibrosis (HF) is a critical marker of advanced-stage chronic liver disease and involves pivotal contributions from hepatic stellate cells (HSCs). Currently, there are no effective treatments for HF. Umbelliferone (7-hydroxycoumarin; UMB) is a natural compound with significant anti-inflammatory, antioxidant and anti-tumor activities. However, its potential efficacy in treating HF has not been studied. The present study explored the protective effects of UMB against HF, targeting the TGF-β1-Smad signaling pathway to explore the underlying mechanisms of UMB. Carbon tetrachloride (CCl_4) was injected intraperitoneally to induce HF in rats and primary HSCs were treated *in vitro* with UMB to investigate the improvement effect of UMB on HF. The levels of fibrosis markers, inflammation, oxidative stress and TGF-β1-Smad signaling pathway in the rat liver tissue and HSCs were detected using hematoxylin and eosin staining, enzyme-linked immunosorbent assay, reverse transcription-quantitative PCR, Cell Counting Kit-8 and western blotting. The improvement in liver histopathology, liver function indexes and fibrosis markers demonstrated that UMB markedly inhibited the CCl_4-induced HF and inflammation in the rats. Additionally, UMB prominently reduced the pro-inflammatory factors and oxidative stress levels. *In vitro*, UMB markedly inhibited primary HSC activation and decreased alpha-smooth muscle actin and collagen I expression. The mechanism experiment proved that UMB inhibited the TGF-β1-Smad signaling pathway and ameliorated HF. The present study was the first to demonstrate, to the best of the authors' knowledge, that UMB might be a promising natural active compound for treating HF. Its therapeutic effect is associated with its modulation of the TGF-β1-Smad signaling pathway.

Correspondence to: Professor Lidao Bao, Department of Pharmacy, Hohhot First Hospital, 150 South Second Ring Road, Hohhot, Inner Mongolia Autonomous Region 010030, P.R. China
E-mail: bzg123420233@163.com

Professor Lan Wu, Mongolia Medical School, Inner Mongolia Medical University, 5 Xinhua Street, Hohhot, Inner Mongolia Autonomous Region 010110, P.R. China
E-mail: bzg123420234@163.com

*Contributed equally

Abbreviations: HF, hepatic fibrosis; HSCs, hepatic stellate cells; UMB, Umbelliferone; CCl_4, carbon tetrachloride; ECM, extracellular matrix; TGF-β1, transforming growth factor beta 1; TNF-α, tumor necrosis factor alpha; α-SMA, alpha smooth muscle actin; TCM, Traditional Chinese medicine; IL, interleukin; AST, aspartate aminotransferase; ALT, alanine aminotransferase; TBA, total bile acids; TBIL, total bilirubin; MDA, malondialdehyde; CAT, catalase; GSH, glutathione; SOD, superoxide dismutase; MMP-1, matrix metalloproteinase 1; TIMP-1, tissue inhibitors of metalloproteinase 1

Key words: hepatic fibrosis, hepatic stellate cell, umbelliferone, inflammation, oxidative stress, transforming growth factor beta 1

Introduction

A substantial number of patients worldwide have chronic liver disease, with some patients eventually progressing to cirrhosis and even liver cancer. The enormous medical costs and loss of labor force among liver disease patients impose a significant burden on socio-economic development (1). Hepatic fibrosis (HF) is a common pathological stage of a number of chronic liver diseases. HF is induced by viral hepatitis, steatohepatitis, metabolic disorders, autoimmune conditions and drug- or toxin-related hepatitis and is a crucial influence on liver disease outcomes (2). HF is a reparative response of the body to chronic liver injury. It is primarily characterized by an imbalance between extracellular matrix (ECM) proliferation and degradation in the liver, leading to abnormal fibrous connective tissue deposition within the liver and liver structure and function disruption (3). Increasing evidence has suggested that

HF is dynamic and reversible (4). However, there are no markedly effective treatment options for HF. Clinically, the main approaches to improving symptoms include lifestyle interventions, liver protection, lipid-lowering therapies and modulating the gut microbiota (5). To date, definitive anti-fibrotic drugs in clinical practice are lacking.

Hepatic stellate cell (HSC) activation is central in the HF process (6) and is a prerequisite for ECM production and a key step in HF formation (7). Quiescent HSCs are responsible for liver regeneration, immune regulation, maintaining sinusoidal circulation and storing vitamin A, providing structural and functional support to the liver, with minimal ECM secretion (8). Continuous stimulation of the liver by chronic inflammation damages Kupffer, bile duct epithelial cells and vascular endothelial cells, which release large amounts of inflammatory factors such as transforming growth factor beta 1 (TGF-β1), tumor necrosis factor alpha (TNF-α), platelet-derived growth factor and connective tissue growth factor, which enter the space of Disse and activate HSCs (9). The activated HSCs transform into myofibroblasts, continuously proliferating and secreting large amounts of ECM components such as collagen I/III and alpha smooth muscle actin (α-SMA), which promote fibrous connective tissue proliferation in the liver and lead to early HF onset (10).

Multiple signaling pathways and cytokines regulate HF pathogenesis, among which the TGF-β1-Smad signaling pathway is a crucial intracellular pathway (11). The TGF-β1-Smad signaling pathway is closely related to HF occurrence and development, including HSC activation and proliferation, ECM deposition, oxidative stress in hepatocytes and autophagy (12). As the pathway is significant in HF formation and progression, blocking it can slow or even reverse HF and effectively reduce liver cancer incidence, thereby decreasing patients' fibrogenesis and carcinogenesis rates (13).

Traditional Chinese medicine (TCM) acts on multiple pathways and targets, which confers a comprehensive advantage for treating diseases with complex pathological mechanisms (14). TCM was recently demonstrated to have good efficacy and promising prospects in HF treatment (15). Umbelliferone (UMB; 7-hydroxycoumarin) is a natural product found in plants of the Rutaceae and Apiaceae families. UMB exhibits various biological and pharmacological activities, including strong antioxidant, anti-inflammatory, anti-diabetic and anti-tumor effects (16). These effects are primarily mediated through the inhibition of oxidative stress and inflammation. Kassim *et al* (17) demonstrated the antioxidant properties of UMB through 1,1-diphenyl-2-picrylhydrazyl radical scavenging. The authors also reported that UMB exhibited effective anti-inflammatory activity in an ovalbumin-induced allergic airway inflammation mouse model.

Reactive oxygen species and oxidative stress can induce hepatocyte damage and death, directly or indirectly leading to HF (18). Notably, UMB inhibited the proliferation of various tumor cells and induced their apoptosis with no significant toxicity to normal cells (19). Therefore, exploiting the anti-inflammatory and antioxidant properties of UMB holds significant potential and hope for effective HF treatment or reducing fibrosis-induced damage. However, there are few reports on the therapeutic effects of UMB on HF and the underlying molecular mechanisms remain undetermined. The present study established a rat model of HF using carbon tetrachloride (CCl_4) and UMB interventions were administered *in vivo* and *in vitro*. It investigated the improvement and reversal of HF by UMB through fibrotic factors, oxidative stress and the TGF-β1-Smad signaling pathway and the effects of UMB on HSC proliferation to provide comprehensive information for improved HF treatment.

Materials and methods

Chemicals and reagents. UMB was from Huahe Medical (purity according to HPLC, 99%). CCl_4 was from Shanghai Aladdin Biochemical Technology Co., Ltd. The enzyme-linked immunosorbent assay (ELISA) kits for TNF-α and IL-6 were from Beijing Solarbio Science & Technology Co., Ltd. The biochemical assay kits for aspartate aminotransferase (AST), alanine aminotransferase (ALT), hydroxyproline, total bile acids (TBA), total bilirubin (TBIL) and hydroxyproline (Hyp) were from Shanghai Enzyme-linked Biotechnology Co., Ltd. The kits for malondialdehyde (MDA), catalase (CAT), glutathione (GSH) and superoxide dismutase (SOD) activity were from Beijing Solarbio Science & Technology Co., Ltd. The Masson and hematoxylin and eosin (H&E) staining kits were from Beijing Solarbio Science & Technology Co., Ltd. TRIzol® and the reverse transcription kit were from Thermo Fisher Scientific, Inc. SYBR Green reagents were from Thermo Fisher Scientific, Inc. The primers were synthesized by Beijing Qingke Biotechnology Co., Ltd. The Cell Counting Kit-8 (CCK-8) kit was from Thermo Fisher Scientific, Inc. The radioimmunoprecipitation assay (RIPA) buffer was from Beijing Solarbio Science & Technology Co., Ltd. The bicinchoninic acid (BCA) assay kit was from Thermo Fisher Scientific, Inc. The primary antibodies against TGF-β1, α-SMA, phosphorylated (p)-Smad2/3, Smad2/3 and β-actin and the horseradish peroxidase (HRP)-conjugated rabbit anti-mouse IgG secondary antibodies were from Cell Signaling Technology, Inc. The ECL chemiluminescence kit was from Beyotime Institute of Biotechnology.

Apparatus. The apparatus used in this study were the PT1020 tissue processor and tissue slicer (Leica Microsystems GmbH), Axio Scan.Z1 Slide Scanner (Zeiss GmbH), Optima XPN-100 Ultracentrifuge (Beckman Coulter, Inc.), automatic biochemical analyzer (Hitachi 7020; Hitachi, Ltd.), Shimadzu UV-1800 UV-Vis Spectrophotometer (Shimadzu Corporation), ABI StepOne Plus real-time PCR system (Applied Biosystems; Thermo Fisher Scientific, Inc.), Tanon-5200 Chemiluminescent Imaging System (Tanon Science and Technology Co., Ltd.), ImageJ (Version 1.48, National Institutes of Health) and GraphPad Prism 9.0 (Dotmatics).

Animal experiments. A total of 32 Specific pathogen-free (SPF)-grade male Sprague-Dawley (SD) rats (age, 6 weeks; weight, 250±30 g) were from the Inner Mongolia Medical University Experimental Animal Center (Hohhot, China). The animals were acclimatized for one week, at a controlled temperature of 22±2˚C and a humidity level of 50±5% in the designated facility, allowed unrestricted access to food and water, and acclimated to alternating 12-h light and dark cycles. No unexpected animal deaths occurred during the

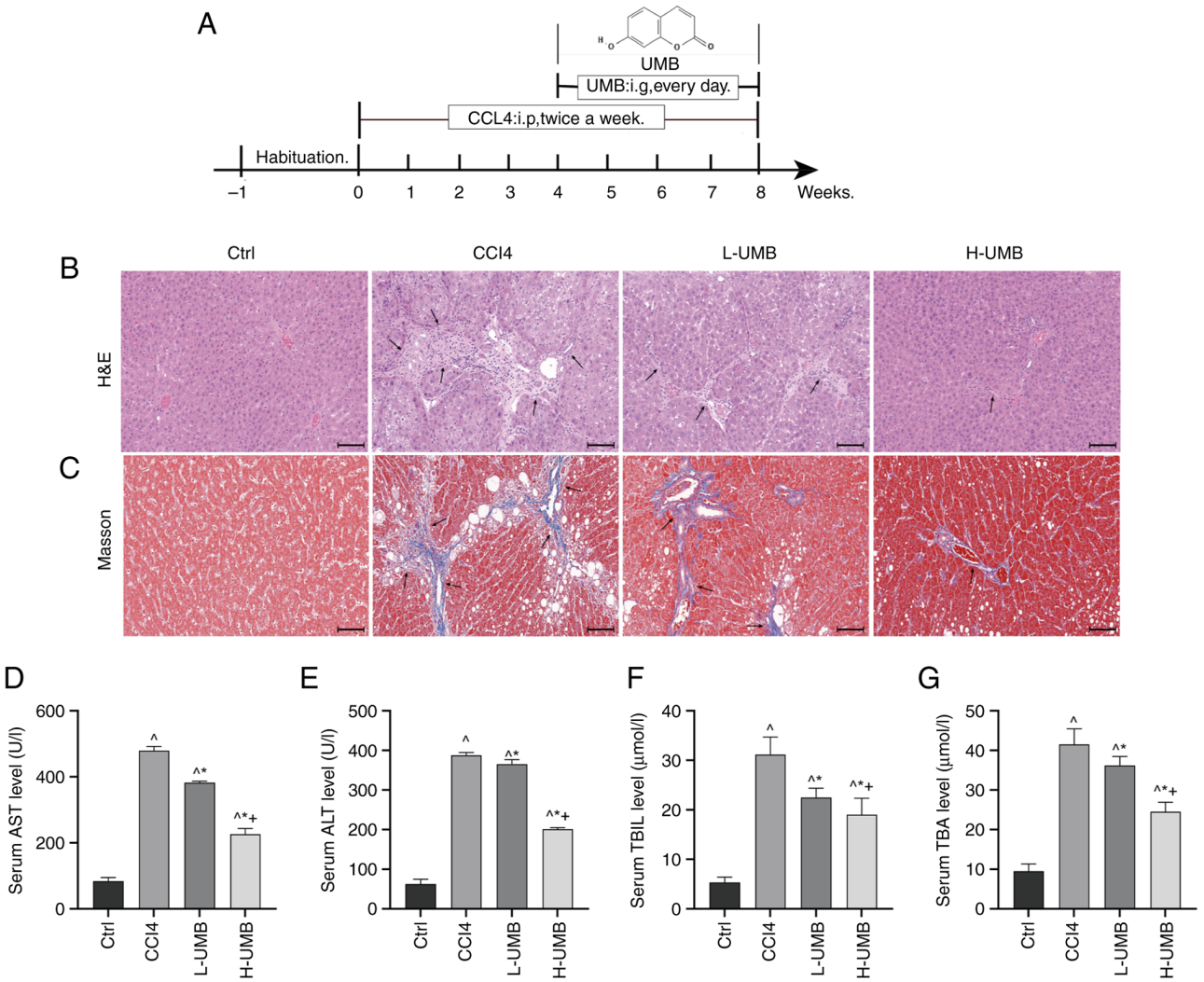

Figure 1. Hepatoprotective effects of UMB in a CCl_4-induced rat HF model. CCl_4-induced rat HF models were treated with 50 or 100 mg/kg/day UMB. (A) The rat model treatment diagram. SD rats were intraperitoneally injected with CCl_4 twice a week and gavaged daily with 50 or 100 mg/kg UMB from week 5 onward. All parameters were analyzed 8 weeks later. (B) H&E and (C) Masson's trichrome staining (magnification, x200). Black arrows indicate damaged liver tissue and fiber cords. Serum levels of AST (D) ALT (E) TBIL (F) and TBA (G) Results are the mean ± SD (n=8). $^{\wedge}$P<0.05 vs. control group; *P<0.05 vs. CCl_4 group; $^{+}$P<0.05 vs. L-UMB. UMB, Umbelliferone; HF, hepatic fibrosis; AST, aspartate aminotransferase; ALT, alanine aminotransferase; TBIL, total bilirubin; TBA, total bile acids; H&E, hematoxylin and eosin; Ctrl, control group; CCl_4, carbon tetrachloride-treated group (model); L-UMB, low-dose UMB treatment (50 mg/kg); H-UMB, high-dose UMB treatment (100 mg/kg).

experiment and all animals were sacrificed in accordance with the approved protocol at the end of the study. Cervical dislocation was employed to ensure a rapid and painless death. The study strictly adhered to humane endpoint criteria to minimize animal suffering, with specific indicators including significant weight loss (>20%), severe behavioral abnormalities, or loss of autonomous feeding and drinking ability. All animal experimental protocols adhered to international ethical guidelines and were approved by the Inner Mongolia Medical University Animal Experiment Ethics Committee (approval no. YKD202201124).

After acclimation, all rats were weighed and randomly divided into four groups (n=8): Control group, CCl_4-treated model group and low and high dose (50 and 100 mg/kg) of UMB co-treated group. The low dose was chosen to reflect a suboptimal therapeutic level, while the high dose was selected to represent a potentially maximal effective dose. A rat model of HF was established by intraperitoneal injection of CCl_4 (3 ml/kg; 40% olive oil solution) twice a week for 8 weeks (with a double dose for the first injection) in the model and UMB treatment groups. The control rats were given olive oil. Starting from day 1 of week 5, UMB (50 or 100 mg/kg) dissolved in 0.5% sodium carboxymethyl cellulose was orally administered to the rats in the UMB treatment groups once daily. The control and model rats received equal volumes of solvent (Fig. 1A). After the final administration, anesthesia was induced and maintained using isoflurane inhalation. The rats were initially anesthetized with 4-5% isoflurane in an induction chamber and then maintained with 1.5-2% isoflurane delivered via a nose cone. Blood samples were collected from the abdominal aortas of each group (5 ml per rat) and the liver tissues were harvested. A portion of the liver tissue was fixed in 4% paraformaldehyde for 24 h at 4˚C and the remainder was stored at -80˚C for further analysis. After procedures, death was confirmed by the absence of a heartbeat, cessation of breathing for at least 5 min and lack of

Table I. Primer sequences used for reverse transcription-quantitative PCR.

Gene	Forward (5'-3')	Reverse (5'-3')
α-SMA	TCCTGACCCTGAAGTATCCG	TCTCCAGAGTCCAGCACAAT
Collagen I	CTGCCGATGTCGCTATCC	CCACAAGCGTGCTGTAGGT
TIMP-1	CCTCTGGCATCCTCTTG	TTGATCTCATAACGCTGGT
MMP-1	ATGCTTAGCCTTCCTTT	CACCCAAGTTGTAGTAGTTTT
β-Actin	CGTTGACATCCGTAAAGACC	GCTAGGAGCCAGGGCAGTA

α-SMA, alpha smooth muscle actin; TIMP-1, tissue inhibitors of metalloproteinase 1; MMP-1, matrix metalloproteinase 1.

pupillary reflexes. If necessary, sacrifice was performed via cervical dislocation.

Primary HSC isolation and culture. The rat livers were digested using collagenase IV and pronase E. The digested cells were filtered through a 200-mesh cell strainer to eliminate undigested tissue. The resulting cell suspension was centrifuged at 40 x g for 3 min at 4˚C and washed three times until the supernatant became clear, thereby removing hepatocytes and collecting the supernatant. The supernatant was centrifuged at 500 x g for 10 min at 4˚C to collect the pellet, which was resuspended in Dulbecco's modified Eagle's medium (DMEM) (Thermo Fisher Scientific, Inc.). The resuspended cells were filtered again through a 200-mesh cell strainer. Then, the pellet was resuspended in 5 ml 40% Percoll solution, overlaid with an equal volume of 12% Percoll solution and topped with 1 ml DMEM. A 30-min centrifugation at 1,150 x g at 4˚C allowed the HSCs to be located between the phosphate-buffered saline (PBS) and 12% Percoll layers. The isolated primary HSCs were cultured for 3 days in the DMEM to promote spontaneous activation before being used in further experiments.

UMB intervention of HSCs. The HSCs ($6x10^4$ cells/ml) were seeded in 96-well plates, treated with 0, 2, 5, 10, or 20 μM UMB, dissolved in dimethyl sulfoxide (DMSO) and cultured for 72 h. The control group was the drug-free group. After 0-, 24-, 48- and 72-h treatment, HSC proliferation was measured using CCK-8. Subsequently, the cells from each group were incubated with the detection reagent at 37˚C for another hour. The HSC proliferation was measured using Shimadzu UV-1800 UV-Vis Spectrophotometer at 450 nm. The hydroxyproline concentration was determined using a commercial kit. At the end of the experiment, the mRNA expression of the fibrosis-related factors TGF-β1 and α-SMA was assessed using reverse transcription-quantitative (RT-q) PCR. The relative TGF-β1, α-SMA, p-Smad2/3 and Smad2/3 protein expression levels were measured using western blotting.

Histopathological examination. The rat liver tissues were fixed in 4% paraformaldehyde for 24 h at 4˚C for pathological analysis. Standard dehydration, xylene-clearing and paraffin-embedding were conducted and 4-μm thick sections were cut with a microtome. The liver tissue sections were deparaffinized and stained with the H&E and Masson staining kits. Finally, the histopathological changes in the liver tissue were observed under a light microscope.

ELISA. Blood samples from each group were centrifuged at 4,000 x g for 10 min at 4˚C to obtain serum samples. The serum TNF-α and IL-6 concentrations were measured using Rat TNF-α ELISA kits (cat. no. Sekr0009) and Rat IL-6 ELISA kits (cat. no. Sekr0005). The ALT, AST, TBIL and TBA concentrations were determined using the automated biochemical analyzer and commercial clinical assay kits (cat. no. Ml059334, cat. no. Ml059335, cat. no. M1224L, cat. no. M122CM48).

Appropriate amounts of liver tissue or HSCs were obtained from each group and the Hyp concentration was measured using a standard commercial kit (cat. no. Ml092986), which is used to assess liver function indicators and evaluate liver function changes. The frozen liver tissues from each group were weighed and homogenized in 0.9 ml ice-cold saline to prepare a 10% homogenate. The homogenate was centrifuged at 4˚C for 10 min at 1,000 x g and the supernatant was collected. The GSH, CAT, SOD and MDA levels in the liver tissue were measured by chemichromatometry according to the directions of the reagent kits (cat. no. BC1170, cat. no. BC0200, cat. no. BC5165, cat. no. BC0020).

Reverse transcription-quantitative (RT-q) PCR. Rat liver tissue or HSCs were homogenized in lysis buffer using a tissue homogenizer. Total RNA was extracted using TRIzol® according to the supplier's instructions. The RNA concentration was measured and RNA purity was assessed by measuring the optical density (OD) at 260/280 nm with a spectrophotometer. The total RNA integrity was evaluated by agarose gel electrophoresis. The total mRNA was reverse-transcribed into cDNA according to the reverse transcription kit instructions. RT-qPCR was performed using SYBR Green with an initial denaturation for 30 sec at 95˚C, followed by 40 cycles of amplification (95˚C for 5 sec and 60˚C for 34 sec), according to the manufacturer's protocol. Each sample was analyzed in triplicate. The internal control was β-actin. The RNA expression levels were calculated using the comparative threshold cycle ($2^{-\Delta\Delta Cq}$) (20) method. Table I presents the RT-qPCR primer sequences.

Western blotting. The rat liver tissues or HSCs were homogenized in RIPA buffer containing protease and phosphatase inhibitors, then centrifuged at 4˚C for 15 min at 8,945 x g to

obtain the supernatant. The total protein concentration was determined using a bicinchoninic acid (BCA) assay kit. A total of 10 μl protein underwent sodium dodecyl sulfate-polyacrylamide gel electrophoresis (10% SDS-PAGE) and then were transferred to a PVDF membrane. The membrane was blocked with skimmed milk for 2 h at 4˚C, then incubated at 4˚C overnight with primary antibodies against TGF-β1 (cat. no. 3711S), p-Smad2/3 (cat. no. 12001C), and Smad2/3 (cat. no. 12460S) (1:1,000 dilution in 3% skimmed milk) to measure the expression of the respective proteins. The internal control was β-actin (1:1,000; cat. no. 4970T). After washing with TBST (0.1% Tween 20), the membrane was incubated for 1 h with secondary antibodies (1:1,000 dilution, cat. no. 7074P2) at room temperature. After washing with TBST, the blots were visualized using the ECL chemiluminescence kit. The protein bands were scanned and detected using the Tanon-5200 chemiluminescent imaging system. Finally, the bands were quantified using ImageJ to calculate the relative expression levels of each protein.

Statistical analysis. The data were analyzed using SPSS (version 26.0). The measurement data are presented as the mean ± standard deviation. Statistical significance was assessed using either the one-way analysis of variance (ANOVA) or Student's t-test, followed by Tukey's post-hoc multiple comparison tests to evaluate differences among groups. $P<0.05$ was considered to indicate a statistically significant difference. The statistical analyses were performed using GraphPad Prism 9.0 (Dotmatics).

Results

UMB alleviates CCl_4-induced liver damage in the rat model. There were no unexpected fatalities in any group throughout the study. The control rats exhibited optimal health, characterized by agility, regular dietary patterns and normal bowel movements. By contrast, the model rats exhibited slightly diminished mental states and signs of irritability. The rats in the treatment group exhibited noticeable improvements compared with the model rats.

Liver tissue abnormalities were identified using H&E staining (21). The analysis revealed that the hepatocytes of the model group had a disorganized arrangement and were accompanied by small and variably sized round vacuoles, along with sporadic inflammatory cell infiltration. The UMB treatment was followed by a notable improvement in hepatocyte integrity and reduced inflammatory infiltration. Notably, the treatment groups exhibited decreased hepatic steatosis, necrosis and collagen deposition, suggesting a restoration towards normal liver architecture (Fig. 1B). The Masson staining results indicated markedly increased perivascular and interstitial fibrosis in the CCl_4-induced rats (22). UMB ameliorated these fibrotic changes (Fig. 1C). Furthermore, the higher dose of UMB (100 mg/kg) was more effective than the lower dose (50 mg/kg), demonstrating that UMB markedly mitigated the CCl_4-induced liver pathology and fibrosis, providing substantial protective and therapeutic benefits.

Effect of UMB on liver function indicators. AST and ALT are critical biomarkers for assessing liver function and are extensively utilized in diagnosing liver damage in clinical settings (23). TBIL and TBA are indicators of cholestasis, reflecting the secretory and excretory capacities of the liver (24). The present study evaluated changes in these liver-associated parameters in CCl_4-induced rats that received 50 and 100 mg/kg UMB. The results demonstrated a statistically significant dose-dependent reduction in AST, ALT, TBIL and TBA levels in the treatment groups compared with the model group ($P<0.05$; Fig. 1D-G). These results suggested that UMB effectively mitigated hepatocyte damage and enhanced liver functionality. Unexpectedly, the data also revealed that UMB might alleviate liver injury-associated bile stasis.

Effects of UMB on inflammation levels. Inflammatory responses activate HSCs, which regulate immune responses by secreting chemokines and cytokines, or transform into myofibroblasts that produce matrix, advancing liver fibrosis progression (25). The inflammatory responses associated with HF in the rats was evaluated using ELISA kits to quantify the serum TNF-α and IL-6 concentrations following UMB treatment. The results demonstrated that UMB significantly decreased the serum TNF-α and IL-6 levels dose-dependently compared with the model group ($P<0.05$; Fig. 2).

Following UMB intervention, a marked reduction in the levels of pro-inflammatory cytokines TNF-α and IL-6 was observed, which associated consistently with the diminished inflammatory cell infiltration evident in liver histopathological analysis. This concordance between cytokine modulation and histopathological findings provided evidence supporting the anti-inflammatory efficacy of UMB to reduce liver damage.

Effects of UMB on liver oxidative stress. Oxidative stress is pivotal in the pathogenesis of liver disorders, markedly contributing to hepatic injury and fibrosis advancement (26). Hepatocytes combat oxidative stress using enzymatic and non-enzymatic antioxidant defenses (27). The prominent enzymatic antioxidants include SOD and CAT, whereas GSH is a crucial non-enzymatic antioxidant (28). Furthermore, MDA levels indicate lipid peroxidation (29). Given its recognized antioxidant capabilities, the present study proposed that UMB might protect rat livers against fibrosis by leveraging these antioxidant mechanisms. This hypothesis was substantiated by evaluating the expression levels of key oxidative stress-associated markers. The results of the present study demonstrated that UMB notably decreased MDA levels and dose-dependently increased GSH, SOD and CAT concentrations significantly compared with the control group ($P<0.05$; Fig. 3). These results highlighted the efficacy of UMB in limiting CCl_4-induced oxidative stress in the liver and mitigating fibrosis, underscoring its potential to preserve liver function by modulating antioxidant enzyme activities.

Effects of UMB on the expression of pro-fibrotic related genes in HF rats. α-SMA and collagen I are pivotal in HSC activation and the ensuing fibrosis process primarily through their roles in ECM synthesis (30). Matrix metalloproteinases (MMPs) and tissue inhibitors of metalloproteinases (TIMPs) regulate ECM remodeling, with MMP-1 and TIMP-1 being crucial for maintaining the balance within the liver matrix (31). The present study aimed to elucidate the mechanism by which

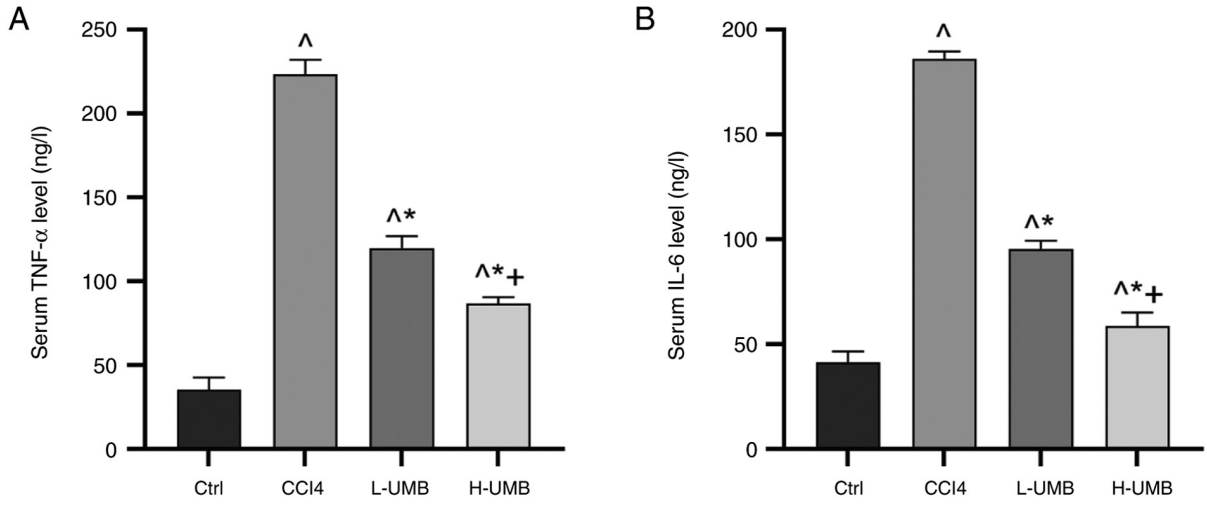

Figure 2. Effects of UMB on inflammation levels in HF rats. CCl_4-induced rat HF models were treated with 50 or 100 mg/kg/day UMB. (A) Serum TNF-α level. (B) Serum IL-6 level. Results are the mean ± SD (n=8). ^P<0.05 vs. control group; *P<0.05 vs. CCl_4 group; +P<0.05 vs. L-UMB. UMB, Umbelliferone; HF, hepatic fibrosis; TNF-α, tumor necrosis factor alpha; IL, interleukin; Ctrl, control group; CCl_4, carbon tetrachloride-treated group (model); L-UMB, low-dose UMB treatment (50 mg/kg); H-UMB, high-dose UMB treatment (100 mg/kg).

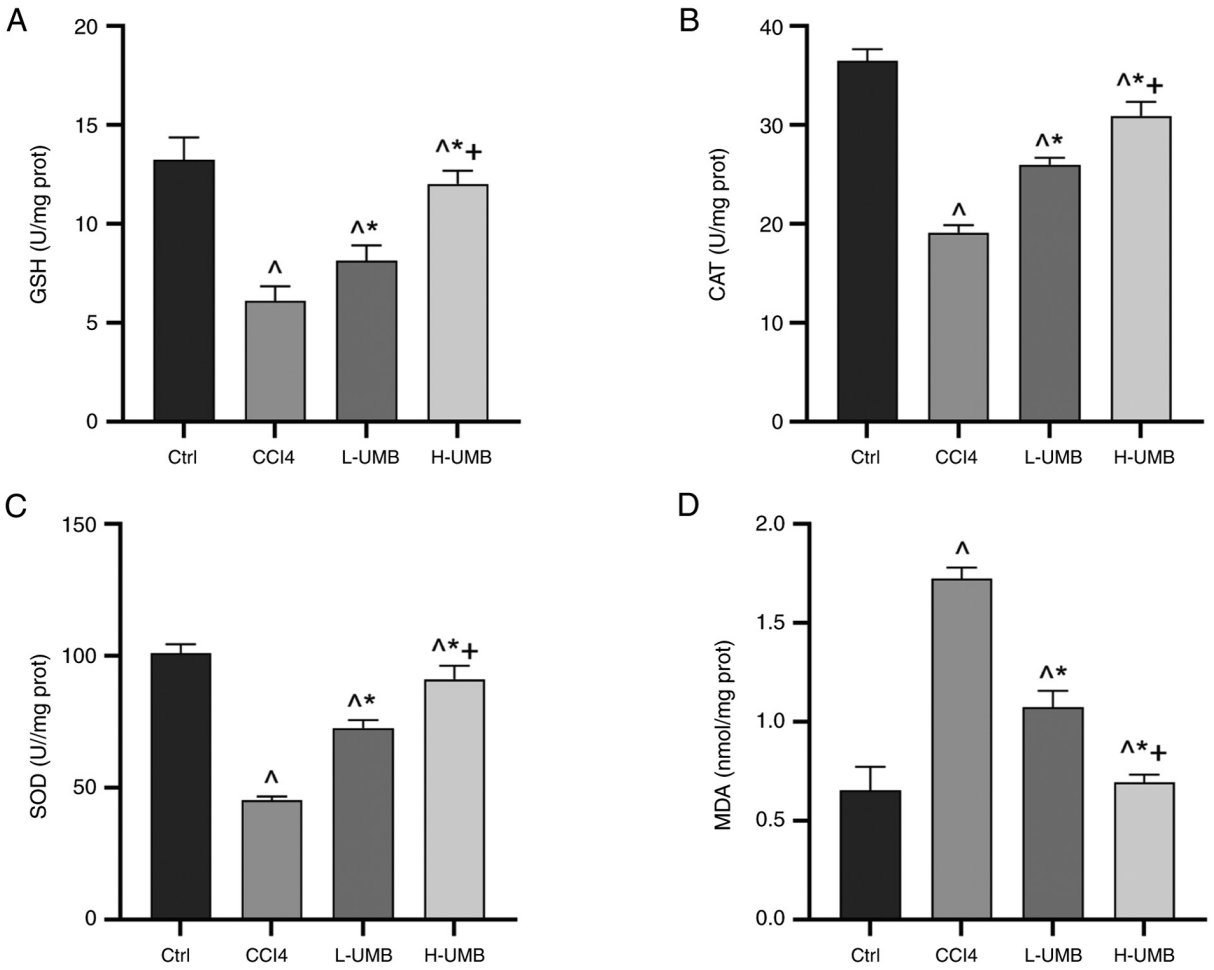

Figure 3. Effects of UMB on liver oxidative stress. CCl_4-induced rat HF models were treated with 50 or 100 mg/kg/day UMB. Liver tissue levels of (A) GSH, (B) CAT, (C) SOD and (D) MDA. Results are the mean ± SD (n=8). ^P<0.05 vs. control group; *P<0.05 vs. CCl_4 group; +P<0.05 vs. L-UMB. UMB, Umbelliferone; HF, hepatic fibrosis; Ctrl, control group; CCl_4, carbon tetrachloride-treated group (model); L-UMB, low-dose UMB treatment (50 mg/kg); H-UMB, high-dose UMB treatment (100 mg/kg); GSH, glutathione; SOD, superoxide dismutase; CAT, catalase; MDA, malondialdehyde.

UMB mitigates HF. The quantitative analysis results of the mRNA expression of these fibrosis-related markers indicated that α-SMA, collagen I and TIMP-1 levels were significantly elevated relative to those of the control group, whereas the

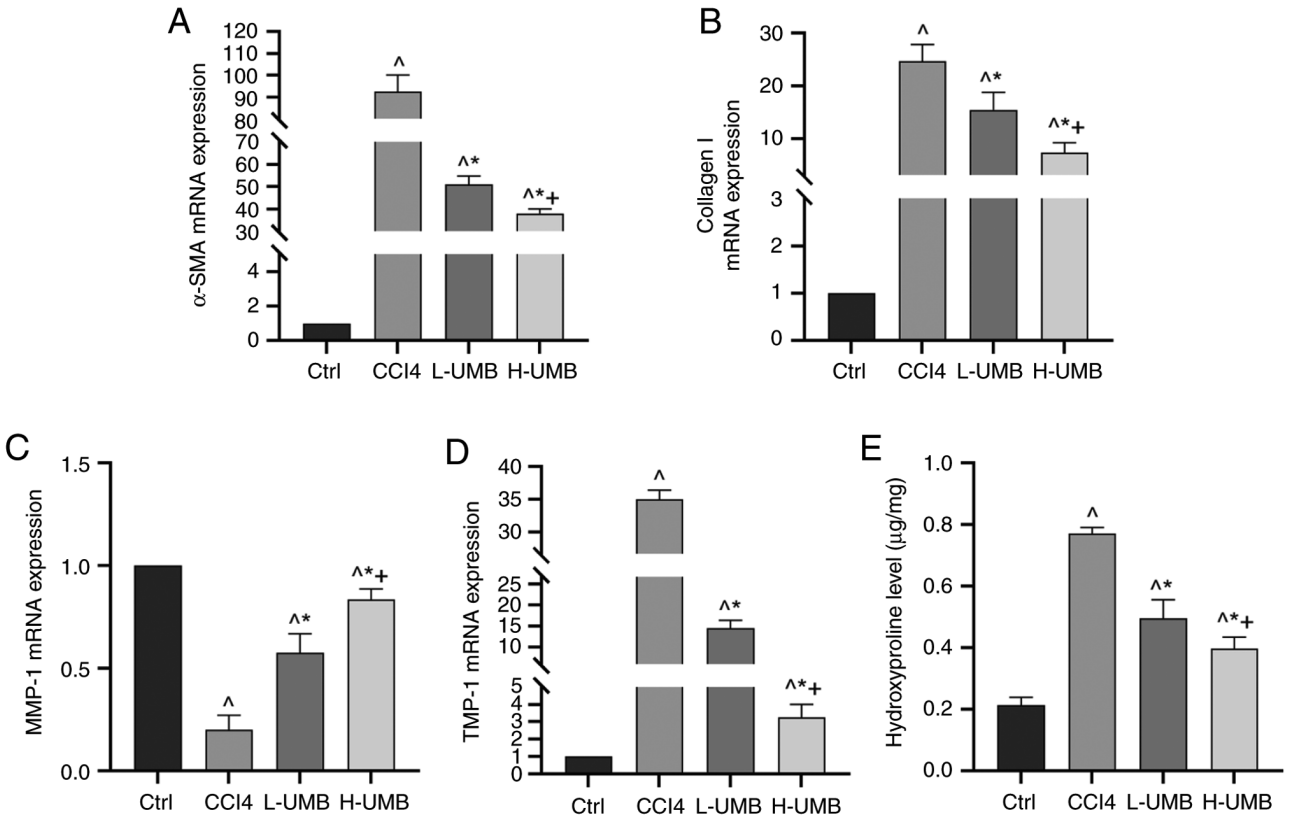

Figure 4. Effects of UMB on expression of pro-fibrotic related genes in HF rats. CCl_4-induced rat HF models were treated with 50 or 100 mg/kg/day UMB. mRNA expression was detected using RT-qPCR. mRNA expression of (A) α-SMA, (B) collagen I, (C) MMP-1 and (D) TIMP-1. (E) Hydroxyproline expression. Results are the mean ± SD (n=8). $^{\wedge}$P<0.05 vs. control group; *P<0.05 vs. CCl_4 group; $^{+}$P<0.05 vs. L-UMB. UMB, Umbelliferone; HF, hepatic fibrosis; RT-qPCR, reverse transcription-quantitative PCR; α-SMA, alpha smooth muscle actin; MMP-1, matrix metalloproteinase 1; TIMP-1, tissue inhibitors of metalloproteinase 1; Ctrl, control group; CCl_4, carbon tetrachloride-treated group (model); L-UMB, low-dose UMB treatment (50 mg/kg); H-UMB, high-dose UMB treatment (100 mg/kg).

model group had markedly reduced MMP-1 levels (P<0.05). Significantly, 50 and 100 mg/kg UMB reversed these changes dose-dependently (P<0.05; Fig. 4A-D). Furthermore, hydroxyproline levels, which indicate collagen deposition, were also decreased significantly in the UMB-treated rat liver tissues, indicating reduced fibrosis (P<0.05; Fig. 4E). These outcomes suggested that UMB substantially reduced pro-fibrotic factor expression and effectively counteracted HF progression.

Effects of UMB on the TGF-β1-Smad2/3 pathway in HF rats. The effects of UMB on HF were assessed by quantifying the TGF-β1, phosphorylated (p-)Smad2/3 and total Smad2/3 protein expression levels in rat liver tissues using western blotting. The results revealed that the model group had markedly elevated TGF-β1 and p-Smad2/3 protein levels compared with the control, suggesting enhanced fibrotic activity. Upon UMB administration, there was a notable dose-dependent decrease in the expression of these proteins, confirming the anti-fibrotic efficacy of UMB (P<0.05). However, the UMB treatment did not significantly alter the total Smad2/3 protein levels, indicating a selective effect of UMB on the phosphorylated forms of Smad proteins (P>0.05; Fig. 5).

UMB inhibits HSC activation and proliferation in vitro. Considering the pivotal role of HSCs in HF onset and advancement, the present study explored whether the beneficial effects of UMB on reducing HF might be due to its capability of suppressing HSC activation. The effects of UMB on HSC proliferation were assessed using the CCK-8 assay, which indicated that UMB significantly limited HSC proliferation in a time- and dose-dependent manner (P<0.05). Notably, the proliferation rates in the 2 and 5 μM UMB-treated groups did not significantly diverge from those of the control group (0 μM) at the 24-h mark, indicating no substantial effect at these lower concentrations (P>0.05; Fig. 6A). The UMB treatment dose-dependently suppressed the α-SMA and collagen I mRNA levels of fibrogenic genes in the HSCs (P<0.05) (Fig. 6B and C). Conversely, an increased UMB concentration corresponded with a significant downtrend in HSC hydroxyproline levels (P<0.05; Fig. 6D). This trend underscored the potential of UMB to effectively mitigate ECM accumulation, thereby impeding HSC proliferation.

Effects of UMB on the TGF-β1-Smad2/3 pathway in HSCs. TGF-β1 is a powerful pro-fibrotic factor essential for activating HSCs, a process pivotal to HF development (32). The present study aimed to delve deeper into the mechanisms through which UMB impedes HSC activation and the resultant fibrosis. Specifically, the present study examined the modulatory effects of UMB on the TGF-β1 signaling pathway. It explored the effects of UMB on the expression of critical proteins in HSCs by administering different doses over different durations.

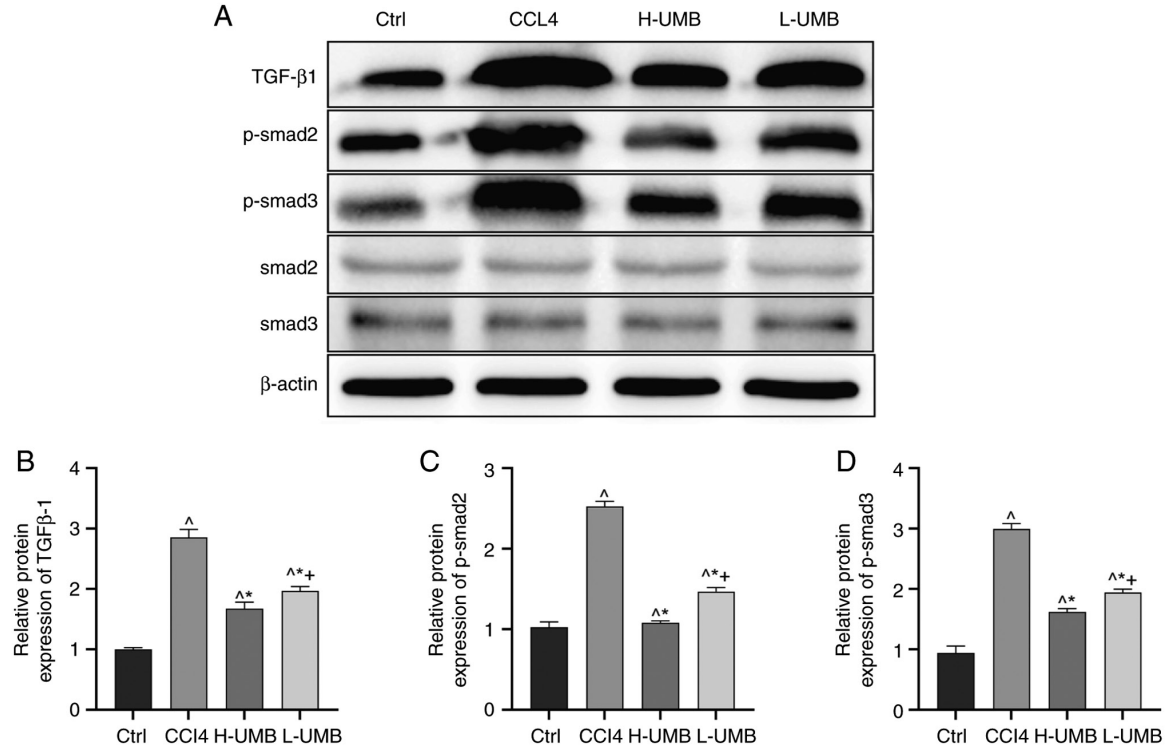

Figure 5. Effects of UMB on the TGF-β1-Smad2/3 pathway in HF rats. CCl_4-induced rat HF models were treated with 50 or 100 mg/kg/day UMB. (A) Western blot measurement of TGF-β1, Smad2, Smad3, p-Smad2 and p-Smad3 protein expression levels. Quantitation of western blot analysis of (B) TGF-β1, (C) p-Smad2 and (D) p-Smad3. Results are the mean ± SD (n=8). $^{\wedge}$P<0.05 vs. control group; *P<0.05 vs. CCl_4 group; $^{+}$P<0.05 vs. L-UMB. UMB, Umbelliferone; Ctrl, control group; CCl_4, carbon tetrachloride-treated group (model); L-UMB, low-dose UMB treatment (50 mg/kg); H-UMB, high-dose UMB treatment (100 mg/kg); p-, phosphorylated; TGF-β1, transforming growth factor beta 1.

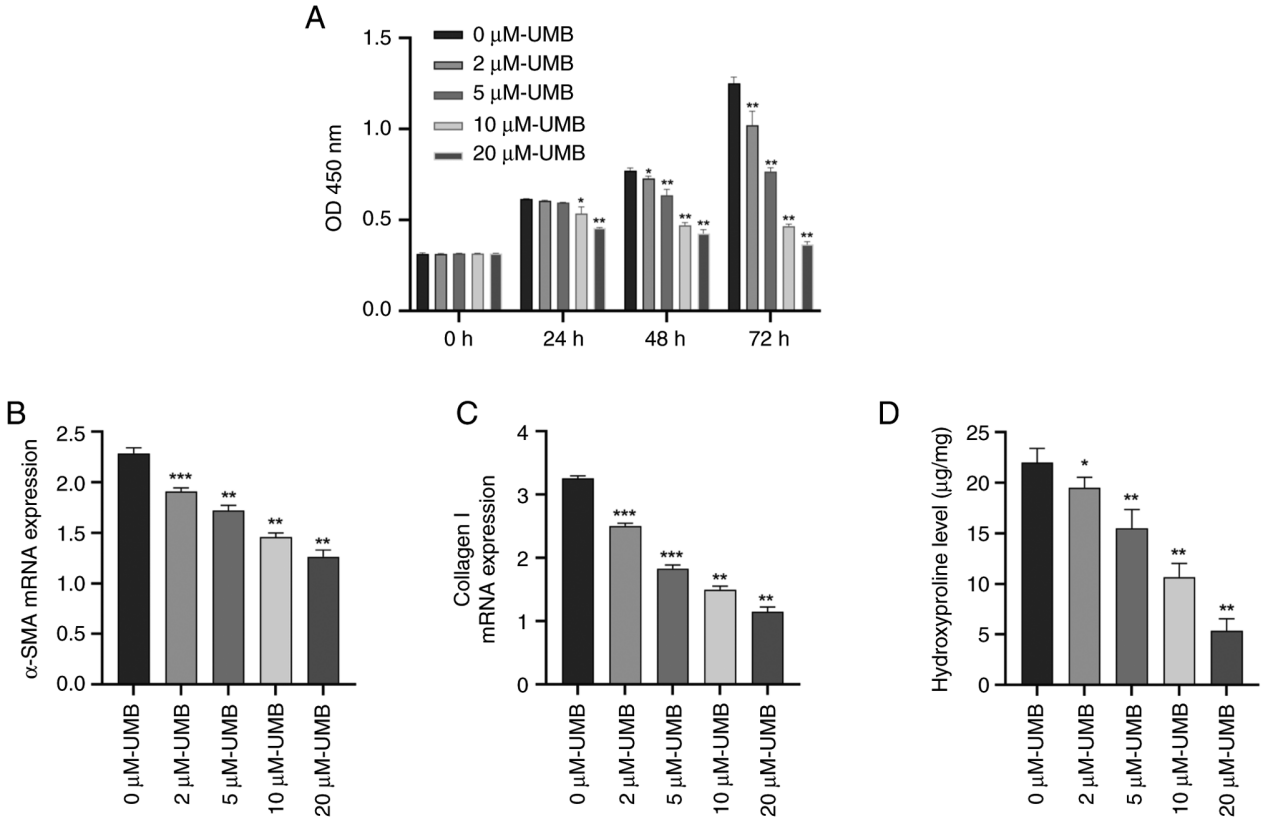

Figure 6. UMB inhibited HSC activation and proliferation *in vitro*. HSCs were treated with 0, 2, 5, 10, or 20 μM UMB dissolved in DMSO and cultured for 72 h. (A) CCK-8 assay measurement of relative cell viability of HSCs. mRNA expression was detected using RT-qPCR. (B) α-SMA mRNA expression. (C) Collagen I mRNA expression. (D) Hydroxyproline expression. Results are the mean ± SD (n=8). *P<0.05, **P<0.01, ***P<0.001 vs. 0 μM UMB. UMB, Umbelliferone; HSCs, hepatic stellate cells; α-SMA, alpha smooth muscle actin.

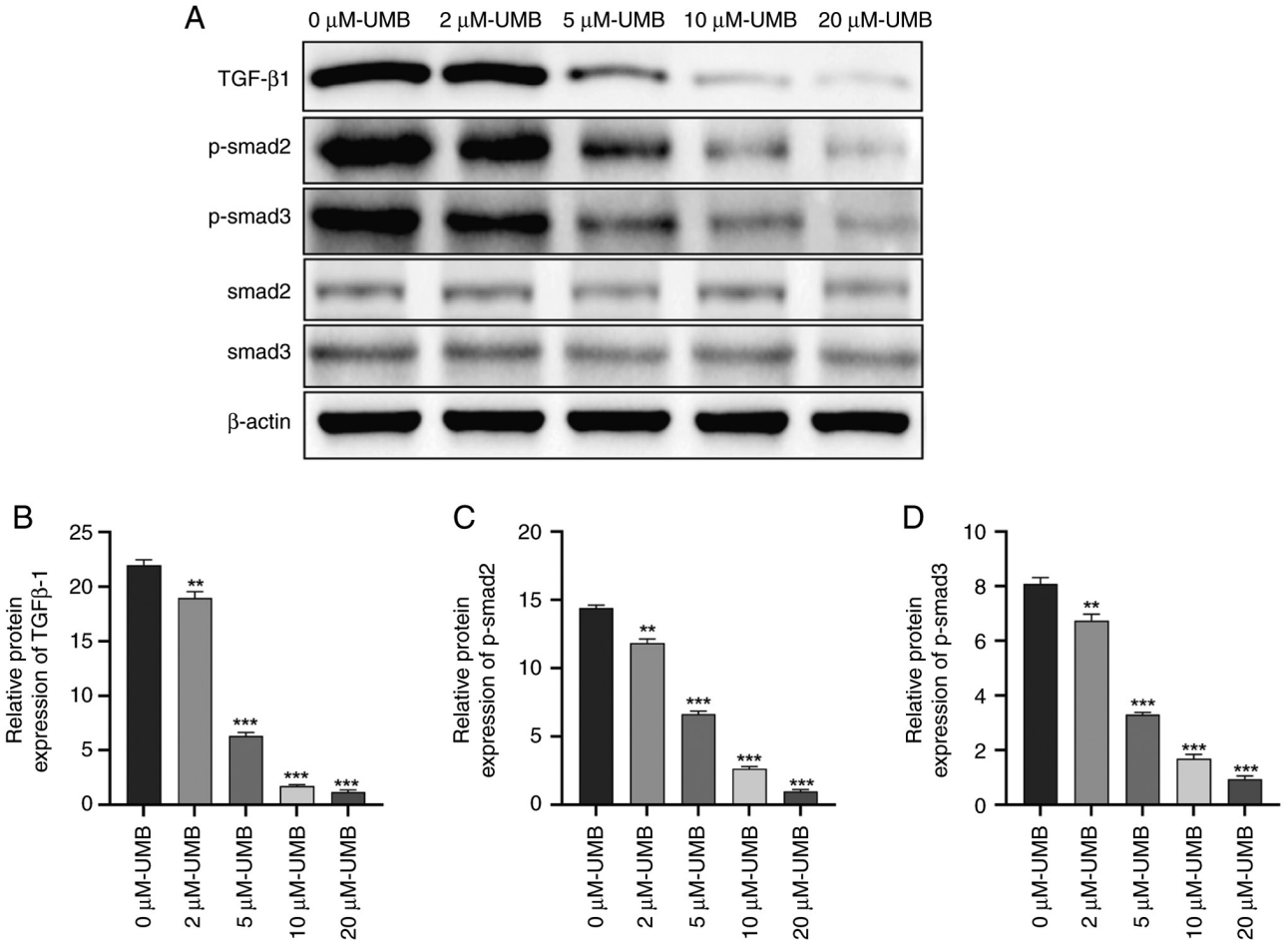

Figure 7. Effects of UMB on the TGF-β1-Smad2/3 pathway in HSCs. HSCs were treated with 0, 2, 5, 10, or 20 μM UMB dissolved in DMSO and cultured for 72 h. (A) Western blot measurement of TGF-β1, Smad2, Smad3, p-Smad2 and p-Smad3 protein expression levels. Quantitation of western blot analysis of (B) TGF-β1, (C) p-Smad2 and (D) p-Smad3. Results are the mean ± SD (n=3). **P<0.01, ***P<0.001 compared with 0 μM UMB. UMB, Umbelliferone; HSCs, hepatic stellate cells; TGF-β1, transforming growth factor beta 1; p-, phosphorylated.

The results demonstrated that the TGF-β1 and p-Smad2/3 expression levels in the HSCs paralleled those in the liver tissue, demonstrating a significant dose-dependent response (P<0.05). Conversely, the total Smad2/3 expression levels were not statistically significantly altered (P>0.05; Fig. 7). These results suggested that UMB potentially modulates the HSC activation state by influencing TGF-β1 and p-Smad2/3 expression, which may be pivotal in HF progression.

Discussion

HF is a common pathological progression in a number of chronic liver diseases, where timely and effective intervention is pivotal for treating these diseases and preventing the onset of cirrhosis and liver cancer (33). In various chronic liver conditions, fibrosis is reversible before it advances to severe cirrhosis. HSCs are specialized mesenchymal cells in the liver that are crucial in normal physiological and pathological processes (34). HSCs triggered by external stimuli transdifferentiate into myofibroblasts, which significantly contribute to ECM accumulation, leading to HF (35). UMB is a natural coumarin from Rutaceae and Apiaceae plants that has demonstrated efficacy in treating a range of acute and chronic conditions due to its wide-ranging biological and pharmacological properties (16). Nevertheless, its effectiveness against HF has been relatively underexplored. The present study investigated the protective effects of UMB on CCl_4-induced HF in rats and its mechanisms on primary cultured HSCs.

Previous studies (36,37) have demonstrated that UMB intervention promoted the normalization of liver cell arrangement in fibrotic rats, accompanied by reduced fibrous tissue and inflammatory cell infiltration. Furthermore, administering 50 and 100 mg/kg UMB in the present study effectively decreased the serum TNF-α, IL-6, ALT, AST, TBIL and TBA levels in the fibrotic models. These observations indicated that UMB may reduce inflammation in liver tissues and mitigate fibrosis-associated damage. Consequently, these results underscored the potential of UMB to slow HF progression and highlighted its significant hepatoprotective effects.

ECM deposition is the hallmark of HF and is pivotal in disease progression. Under pathological conditions, TGF-β1 overexpression catalyzes ECM accumulation (38). In this context, α-SMA and collagen I are critical biomarkers for assessing ECM deposition (39). The interplay between MMPs and their inhibitors is essential for ECM remodeling, with MMP-1 and TIMP-1 being particularly significant (40). MMP-1 is a principal enzyme in collagen I and III degradation

and facilitates ECM breakdown (41). Strategic modulation that increases MMP-1 and decreases TIMP-1 markedly promotes ECM degradation, mitigating HF in rat models (42). In the present study, the fibrotic model rats exhibited elevated levels of pro-fibrotic factors (TGF-β1, α-SMA and TIMP-1) and notably reduced MMP-1 expression. Conversely, these trends were reversed in the UMB-treated groups. In summary, the findings demonstrated that UMB exerts a dose-dependent reduction in the expression of fibrotic gene markers. For example, curcumin appears to directly inhibit HSCs activation, as evidenced by its ability to downregulate key fibrotic markers such as α-SMA and collagen I, consistent with previous studies (25). In addition, Berberine may also modulate the hepatic microenvironment through its anti-inflammatory properties, reducing the release of pro-inflammatory cytokines and regulating Kupffer cell activity, thereby indirectly attenuating HSC activation (17). These dual mechanisms highlight the multifaceted anti-fibrotic potential of UMB, suggesting that its therapeutic effects are probably mediated through a combination of direct actions on HSCs and broader modulation of the liver microenvironment.

Oxidative stress represents an imbalance between oxidative mechanisms and antioxidant processes in the body, contributing significantly to the development of conditions such as atherosclerosis and fibrosis (43). Oxidative stress is pivotal in HF, where excess free radicals inflict chemical damage on lipids, proteins and carbohydrates (44). This damage disrupts cellular metabolism, leading to liver cell injury and fibrosis progression (45). The present study delved into the effects of oxidative stress on HF by analyzing oxidative stress markers. The rats with fibrosis exhibited reduced GSH, CAT and SOD levels and markedly increased MDA, which indicated lipid peroxidation caused by free radicals. Conversely, UMB markedly increased antioxidant levels and significantly reduced MDA levels, demonstrating its potential protective effects against CCl_4-induced HF. These results underscored the antioxidative properties of UMB in counteracting HF.

TGF-β1 is pivotal in promoting fibrosis and is closely linked to HF onset and progression. As downstream effectors of TGF-β1, Smad2/3 proteins enhance TGF-β1-induced HF through their phosphorylation processes. TGF-β1 activates the Smad protein signaling cascade upon binding to its specific receptors on the liver cell surface (45). This activation triggers apoptosis and accelerates ECM synthesis while concurrently inhibiting its degradation, thereby intensifying HF (11). Consequently, inhibiting the TGF-β1-Smad signaling pathway presents a dual therapeutic advantage: it reduces ECM formation and attenuates HF (46). The present study revealed that the NF-κB pathway acted in concert with TGF-β1 signaling and pharmacological inhibition of NF-κB markedly attenuated TGF-β1-mediated hepatic fibrosis (47). In addition, there is functional interplay between autophagy and TGF-β1 signaling, showing that augmented autophagy alleviated TGF-β1-driven hepatic fibrosis through the clearance of impaired organelles and protein aggregates (48). The experimental results supported this mechanism, demonstrating significantly elevated TGF-β1 and p-Smad2/3 levels in the model group, which UMB treatment substantially reversed. The reduction in p-Smad2/3 levels primarily reflected the inhibition of the TGF-β1 pathway. However, UMB can modulate inflammatory pathways, oxidative stress and other fibrotic signaling cascades, which may synergistically contribute to its overall antifibrotic effects.

Upon liver damage, the injured epithelial cells and fibrotic tissues activate HSCs, prompting their transformation into a myofibroblast phenotype that produces significant quantities of ECM (49). This shift from balanced ECM synthesis to degradation fosters scar tissue development, culminating in HF (50). *In vitro* studies have demonstrated that UMB inhibits HSC proliferation and reduces hydroxyproline production, decreasing the TGF-β1, α-SMA, collagen I and p-Smad2/3 expression levels in the supernatant of these cells. This evidence suggests that UMB effectively prevents TGF-β1 activation, halts HSC conversion into contractile myofibroblasts and suppresses ECM component secretion (51). Consequently, UMB appears to mitigate inflammatory damage in liver cells, inhibit HSC activation and decrease fibrogenic factor synthesis and secretion by inhibiting the TGF-β1-Smad signaling pathway, thereby offering a promising intervention for HF.

The present study demonstrated that UMB effectively reversed HF by modulating the TGF-β1-Smad signaling pathway and its associated factors, underscoring its capacity to halt fibrosis through several pathways and targets. The mechanism by which UMB intervenes in HF appears to involve TGF-β1-Smad pathway regulation through the inhibition of Smad2/3 protein phosphorylation and mRNA expression. Consequently, this inhibition suppresses HSC activation and proliferation, manages collagen metabolism and decreases oxidative stress in liver tissue. These regulatory effects contribute to reversing HF progression, offering innovative perspectives and methodologies for TCM treatments and the development of new clinical drugs.

Acknowledgements

Not applicable.

Funding

The present study was funded by The Natural Science Foundation of China (grant nos. 82160794 and 82160703); Major Project of Natural Science Foundation of Inner Mongolia Autonomous Region (grant no. 2023ZD15); Science and Technology Program of the Joint Fund of Scientific Research for the Public Hospitals of Inner Mongolia Academy of Medical Sciences (grant nos. 2024GLLH0290 and 2024GLL H0404); Program for Young Talents of Science and Technology in Universities of Inner Mongolia Autonomous Region (grant no. NJYT23114); Key Program of Inner Mongolia Medical University (grant no. YKD2022ZD013); Health Science and Technology Program of Inner Mongolia Health Commission (grant nos. 202201238 and 202202158); PhD Initial Funding Project of the Affiliated Hospital of Inner Mongolia Medical University (grant no. NYFY BS 202120); Hohhot Municipal Health and Wellness Young Talent Technology Project (grant nos. 2023012); Inner Mongolia Autonomous Region Health and Wellness Traditional Chinese Medicine (Mongolian Medicine) Technology Program Project (grant no. ZMY2023201); Standardization Project of Mongolian Medicine in Inner Mongolia Autonomous Region (grant no. 2023MB020); Inner

Mongolia Autonomous Region Traditional Chinese Medicine (Mongolian Medicine) Young and Middle-aged Leading Talent Cultivation Project (grant no. 2022RC011); Hohhot Municipal Science and Technology Program Project (grant no. 2023SHE24); Special Fund for Science and Technology: Central Guidance Fund for Local Science and Technology Development (grant no. ZY20200071).

Availability of data and materials

The data generated in the present study may be requested from the corresponding author.

Authors' contributions

LB and LW conceived and designed the research; LL, ZD, YZ, ZS and WY performed the experiments and analyzed the data. LB drafted the manuscript. LL and ZD confirm the authenticity of all the raw data. All authors read and approved the final version of the manuscript.

Ethics approval and consent to participate

All experiments in the present study were approved by The Ethics Committee of Inner Mongolia Medical University (Hohhot, China; approval no. YKD202201124).

Patient consent for publication

Not applicable.

Competing interests

The authors declare that they have no competing interests.

References

1. Pimpin L, Cortez-Pinto H, Negro F, Corbould E, Lazarus JV, Webber L and Sheron N; EASL HEPAHEALTH Steering Committee: Burden of liver disease in Europe: Epidemiology and analysis of risk factors to identify prevention policies. J Hepatol 69: 718-735, 2018.
2. Caligiuri A, Gentilini A, Pastore M, Gitto S and Marra F: Cellular and molecular mechanisms underlying liver fibrosis regression. Cells 10: 2759, 2021.
3. Dawood RM, El-Meguid MA, Salum GM and El Awady MK: Key players of hepatic fibrosis. J Interferon Cytokine Res 40: 472-489, 2020.
4. Khanam A, Saleeb PG and Kottilil S: Pathophysiology and treatment options for hepatic fibrosis: Can it be completely cured? Cells 10: 1097, 2021.
5. Friedman SL: Hepatic fibrosis-overview. Toxicology 254: 120-129, 2008.
6. Ezhilarasan D, Sokal E and Najimi M: Hepatic fibrosis: It is time to go with hepatic stellate cell-specific therapeutic targets. Hepatobiliary Pancreat Dis Int 17: 192-197, 2018.
7. Huang Y, Deng X and Liang J: Modulation of hepatic stellate cells and reversibility of hepatic fibrosis. Exp Cell Res 352: 420-426, 2017.
8. Zhang X, Zeng Y, Zhao L, Xu Q, Miao D and Yu F: Targeting hepatic stellate cell death to reverse hepatic fibrosis. Curr Drug Targets 24: 568-583, 2023.
9. Albanis E and Friedman SL: Hepatic fibrosis. Pathogenesis and principles of therapy. Clin Liver Dis 5: 315-334. v-vi, 2001.
10. Brenner DA, Waterboer T, Choi SK, Lindquist JN, Stefanovic B, Burchardt E, Yamauchi M, Gillan A and Rippe RA: New aspects of hepatic fibrosis. J Hepatol 32 (1 Suppl): S32-S38, 2000.
11. Gressner AM, Weiskirchen R, Breitkopf K and Dooley S: Roles of TGF-beta in hepatic fibrosis. Front Biosci 7: d793-d807, 2002.
12. Hu HH, Chen DQ, Wang YN, Feng YL, Cao G, Vaziri ND and Zhao YY: New insights into TGF-β/Smad signaling in tissue fibrosis. Chem Biol Interact 292: 76-83, 2018.
13. Xu F, Liu C, Zhou D and Zhang L: TGF-β/SMAD pathway and its regulation in hepatic fibrosis. J Histochem Cytochem 64: 157-167, 2016.
14. Smith ME and Bauer-Wu S: Traditional Chinese medicine for cancer-related symptoms. Semin Oncol Nurs 28: 64-74, 2012.
15. Shan L, Liu Z, Ci L, Shuai C, Lv X and Li J: Research progress on the anti-hepatic fibrosis action and mechanism of natural products. Int Immunopharmacol 75: 105765, 2019.
16. Kornicka A, Balewski Ł, Lahutta M and Kokoszka J: Umbelliferone and its synthetic derivatives as suitable molecules for the development of agents with biological activities: A review of their pharmacological and therapeutic potential. Pharmaceuticals (Basel) 16: 1732, 2023.
17. Kassim NK, Rahmani M, Ismail A, Sukari MA, Ee GC, Nasir NM and Awang K: Antioxidant activity-guided separation of coumarins and lignan from Melicope glabra (Rutaceae). Food Chem 139: 87-92, 2013.
18. Hassanein EHM, Hader HF, Elmansy RA, Seleem HS, Elfiky M, Mohammedsaleh ZM, Ali FEM and Abd-Elhamid TH: Umbelliferone alleviates hepatic ischemia/reperfusion-induced oxidative stress injury via targeting Keap-1/Nrf-2/ARE and TLR4/NF-κB-p65 signaling pathway. Environ Sci Pollut Res Int 28: 67863-67879, 2021.
19. Yu SM, Hu DH and Zhang JJ: Umbelliferone exhibits anticancer activity via the induction of apoptosis and cell cycle arrest in HepG2 hepatocellular carcinoma cells. Mol Med Rep 12: 3869-3873, 2015.
20. Livak KJ and Schmittgen TD: Analysis of relative gene expression data using real-time quantitative PCR and the 2(-Delta Delta C(T)) Method. Methods 25: 402-408, 2001.
21. Vázquez JJ: Ground-glass hepatocytes: light and electron microscopy. Characterization of the different types. Histol Histopathol 5: 379-386, 1990.
22. Iezzoni JC: Diagnostic histochemistry in hepatic pathology. Semin Diagn Pathol 35: 381-389, 2018.
23. Sharma P: Value of liver function tests in cirrhosis. J Clin Exp Hepatol 12: 948-964, 2022.
24. Farooqui N, Elhence A and Shalimar: A current understanding of bile acids in chronic liver disease. J Clin Exp Hepatol 12: 155-173, 2022.
25. Koyama Y and Brenner DA: Liver inflammation and fibrosis. J Clin Invest 127: 55-64, 2017.
26. Finkel T: Oxidant signals and oxidative stress. Curr Opin Cell Biol 15: 247-254, 2003.
27. Sánchez-Valle V, Chávez-Tapia NC, Uribe M and Méndez-Sánchez N: Role of oxidative stress and molecular changes in liver fibrosis: A review. Curr Med Chem 19: 4850-4860, 2012.
28. Foyer CH and Noctor G: Redox homeostasis and antioxidant signaling: A metabolic interface between stress perception and physiological responses. Plant Cell 17: 1866-1875, 2005.
29. Tsikas D: Assessment of lipid peroxidation by measuring malondialdehyde (MDA) and relatives in biological samples: Analytical and biological challenges. Anal Biochem 524: 13-30, 2017.
30. Li Y, Fan W, Link F, Wang S and Dooley S: Transforming growth factor β latency: A mechanism of cytokine storage and signalling regulation in liver homeostasis and disease. JHEP Rep 4: 100397. 2022.
31. Naim A, Pan Q and Baig MS: Matrix metalloproteinases (MMPs) in liver diseases. J Clin Exp Hepatol 7: 367-372, 2017.
32. Dewidar B, Meyer C, Dooley S and Meindl-Beinker AN: TGF-β in hepatic stellate cell activation and liver fibrogenesis-updated 2019. Cells 8: 1419, 2019.
33. Dhar D, Baglieri J, Kisseleva T and Brenner DA: Mechanisms of liver fibrosis and its role in liver cancer. Exp Biol Med (Maywood) 245: 96-108, 2020.
34. Tsuchida T and Friedman SL: Mechanisms of hepatic stellate cell activation. Nat Rev Gastroenterol Hepatol 14: 397-411, 2017.
35. Zhang M, Serna-Salas S, Damba T, Borghesan M, Demaria M and Moshage H: Hepatic stellate cell senescence in liver fibrosis: Characteristics, mechanisms and perspectives. Mech Ageing Dev 199: 111572, 2021.
36. Mahmoud AM, Hozayen WG, Hasan IH, Shaban E and Bin-Jumah M: Umbelliferone ameliorates CCl4-induced liver fibrosis in rats by upregulating PPARγ and attenuating oxidative stress, inflammation, and TGF-β1/Smad3 signaling. Inflammation 42: 1103-1116, 2019.

37. Sim MO, Lee HI, Ham JR, Seo KI, Kim MJ and Lee MK: Anti-inflammatory and antioxidant effects of umbelliferone in chronic alcohol-fed rats. Nutr Res Pract 9: 364-369, 2015.
38. Zhang M and Zhang ST: Cells in fibrosis and fibrotic diseases. Front Immunol 11: 1142, 2020.
39. Schuppan D, Ashfaq-Khan M, Yang AT and Kim YO: Liver fibrosis: Direct antifibrotic agents and targeted therapies. Matrix Biol 68-69: 435-451, 2018.
40. Cui N, Hu M and Khalil RA: Biochemical and biological attributes of matrix metalloproteinases. Prog Mol Biol Transl Sci 147: 1-73, 2017.
41. Arakaki PA, Marques MR and Santos MC: MMP-1 polymorphism and its relationship to pathological processes. J Biosci 34: 313-320, 2009.
42. Iredale JP: Tissue inhibitors of metalloproteinases in liver fibrosis. Int J Biochem Cell Biol 29: 43-54, 1997.
43. Gorrini C, Harris IS and Mak TW: Modulation of oxidative stress as an anticancer strategy. Nat Rev Drug Discov 12: 931-947, 2013.
44. Li S, Tan HY, Wang N, Zhang ZJ, Lao L, Wong CW and Feng Y: The role of oxidative stress and antioxidants in liver diseases. Int J Mol Sci 16: 26087-26124, 2015.
45. Baghy K, Iozzo RV and Kovalszky I: Decorin-TGFβ axis in hepatic fibrosis and cirrhosis. J Histochem Cytochem 60: 262-268, 2012.
46. Meng XM, Nikolic-Paterson DJ and Lan HY: TGF-β: the master regulator of fibrosis. Nat Rev Nephrol 12: 325-338, 2016.
47. Wang K, Fang S, Liu Q, Gao J, Wang X, Zhu H, Zhu Z, Ji F, Wu J, Ma Y, *et al*: TGF-β1/p65/MAT2A pathway regulates liver fibrogenesis via intracellular SAM. EBioMedicine 42: 458-469, 2019.
48. Filali-Mouncef Y, Hunter C, Roccio F, Zagjou S, Dupont N, Primard C, Proikas-Cezann T and Reggiori F: The ménage à trois of autophagy, lipid droplets and liver disease. Autophagy 18: 50-72, 2022.
49. De Oliveira da Silva B, Ramos LF and Moraes KCM: Molecular interplays in hepatic stellate cells: Apoptosis, senescence, and phenotype reversion as cellular connections that modulate liver fibrosis. Cell Biol Int 41: 946-959, 2017.
50. Tacke F and Weiskirchen R: Update on hepatic stellate cells: Pathogenic role in liver fibrosis and novel isolation techniques. Expert Rev Gastroenterol Hepatol 6: 67-80, 2012.
51. Weiskirchen R and Tacke F: Cellular and molecular functions of hepatic stellate cells in inflammatory responses and liver immunology. Hepatobiliary Surg Nutr 3: 344-363, 2014.

Copyright © 2025 Liang et al. This work is licensed under a Creative Commons Attribution-NonCommercial-NoDerivatives 4.0 International (CC BY-NC-ND 4.0) License.